NMR relaxation studies in doped poly-3-methylthiophene

K. Jugeshwar Singh, W. G. Clark, G. Gaidos, A. P. Reyes, P. Kuhns, J. D. Thompson, R. Menon, and K. P. Ramesh

Phys. Rev. B **91**, 174421 — Published 19 May 2015

DOI: 10.1103/PhysRevB.91.174421

NMR relaxation studies in doped poly-3-methylthiophene

K. Jugeshwar Singh[1*], W.G. Clark[2], G. Gaidos[2], A.P. Reyes[3], P. Kuhns[3], J. D. Thompson[4], R. Menon[1] and K.P. Ramesh[1*]

[1] Department of Physics, Indian Institute of Science, Bangalore-560012, India.
[2]Department of Physics and Astronomy, UCLA, Los Angeles, California 90095-1547, USA
[3]National High Magnetic Field Laboratory, Tallahassee, Florida 32310, USA
[4]Los AlamosNationalLaboratory, Los Alamos, NM 87545, USA

*Corresponding Authors: jshwar@physics.iisc.ernet.in; kpramesh@physics.iisc.ernet.in

Abstract:NMR relaxation rates ($1/T_1$), magnetic susceptibility, and electrical conductivity studies in doped poly-3-methylthiophene (p3MT) are reported in this study. The magnetic susceptibility data show the contributions from both Pauli and Curie spins, with the size of the Pauli term depending strongly on the doping level. Proton and Fluorine NMR relaxation rate has been studied as a function of temperature (3-300 K) and field (for protons at 0.9 T, 9.0 T, 16.4 T, 23.4 T and for fluorine 9.0 T). The temperature dependence of T_1 is classified into three regimes: (a) for $T \langle (g\mu_B \mathbf{B}/2k_B)$ - relaxation mechanism follows modified Korringa relation due to EEI and disorder. ^{1}H-T_1 is due to the electron-nuclear dipolar interaction in addition to the contact term. (b) for intermediate temperature range $(g\mu_B \mathbf{B}/2k_B) \langle T \langle T_{BPP}$, the temperature where the contribution from the reorientation motion to the T_1 is insignificant) - relaxation mechanism is via spin diffusion to the paramagnetic centers (SDPC) and (c) in the high temperature regime and atlow Larmor frequency–the relaxation follows the modified Bloembergen, Purcell and Pound (BPP) model.T_1 data analysis has been carried out in the light of these models depending upon the temperature and frequency range of study.Fluorine relaxation data has been analyzed and attributed to the PF_6 reorientation. The cross relaxation among the ^{1}H and ^{19}F nuclei has been observed in the entire temperature range suggesting the role of magnetic dipolar interaction modulated by the reorientation of the symmetric molecular sub-groups.The data analysis shows that the enhancement in Korringa ratio is more in less conducting sample. Intra and inter chain hopping of charge carriers is found to be a dominant relaxation mechanism at low temperature. Frequency dependence of T_1^{-1} and on temperature shows that at low temperature [$T \langle (g\mu_B \mathbf{B}/2k_B)$] the system shows 3-Dimension (3-D) and changes to quasi 1-Dimension (q1-D) at high temperature. Moreover a good correlation between electrical conductivity, magnetic susceptibility and NMR T_1 data has been observed.

PACS number: 73.61.Ph and 76.60.-k

1. INTRODUCTION

Conducting polymers in general are of great deal of interest for the past three decades due to fundamental scientific reasons and also for the development of new materials for modern technology. Despite these properties, certain basic questions concerning their electronic structure, nature of the charge carriers and the dimensionality of the charge transport are still under debate. Poly 3-alkylthiophenes are an unusual class of polymers among many other conjugated polymers due to their conductivity, processibility, environmental stability etc.

Solid state nuclear magnetic resonance (NMR) is very sensitive tool to study the microscopic details of charge and spin distributions and their dynamics, through Knight shifts and relaxation behavior. These studies along with susceptibility, charge transport give a comprehensive insight into the conducting polymer.

Nuclear magnetic resonance spin lattice relaxation rate (T_1^{-1}) studies have been widely used to investigate the charge transport mechanism in both conventional[1] and novel organic[2], polymeric[3] and ceramic conductors[4,5]. In usual metals, the delocalized charge carriers dominate the relaxation mechanism via the carrier dynamics due to the hyperfine interactions; whereas in disordered systems like glasses the reorientation of the symmetric molecular groups is the main relaxation mechanism (at high temperatures), while at very low temperatures (T) the role of two-level system is also observed[6-8]. The relaxation phenomena in several systems follows a universal behavior like many other properties e.g. linear dependence of specific heat with temperature and quadratic variation of thermal conductivity upto a few Kelvin are explained on the basis of the phenomenological model proposed by Anderson[9] and Phillips[10] which is commonly known as two level systems.

The well-known Korringa relaxation mechanism[11], which occurs over a wide range of T in conventional metals, is due to the s-contact hyperfine interaction, which couples the nuclear spins with the conduction electrons. It results in a linear relation between T_1^{-1} and T that is independent of the magnetic field (magnitude B). The result is often expressed as the Korringa relation $K_r=1/(\kappa^2 T_1 T)$, where $K_r = \frac{4\pi k_B}{\hbar}\left(\frac{\gamma_e^2}{\gamma_n^2}\right)$ is the Korringa constant, κ is the Knight shift, k_B is the Boltzmann constant, $\hbar$ is the Planck constant, and γ_e and γ_n are respectively the conduction electron and nuclear gyromagnetic ratios. A deviation from this value of κ is often attributed to the contributions from electron-electron interactions (EEI). Also when $K_r < 1$, the stoner enhancement due to the uniform susceptibility can alter the value of κ[12]. Hence the correction to the susceptibility due to disorder, which in turn affects the Korringa ratio, has to be considered in the data analysis. For example, in Si:P the measured $(T_1T)^{-1}$ values are nearly three orders of magnitude larger than the free electron values[12]. It is important to note that both the Stoner enhancement and disorder contribute to this variation in Korringa ratio. Also, a change in the correlation time (τ_e) for the electronic motion with temperature and a broad distribution in τ_e from sample inhomogeneities and other sources can generate a

dependence of the conduction electron contribution to $(T_1T)^{-1}$ on both **B** and temperature which deviates strongly from the Korringa relation model.

These results suggest that it is quite important to know how disorder and EEI modify the Korringa relation in various systems. In this context conducting polymers are useful candidates since the carrier density and disorder can be varied substantially. Furthermore the intrinsic q1-D also makes it rather interesting to investigate how these factors come into play in the relaxation mechanisms. The earlier relaxation studies in conducting polymers like polypyrrole[13], polyacetylene[14], polyaniline[15] and organic conducting salts like TTF-TCNQ[16], Fluoroanthene$_2$(PF_6)[17], (pyrene)$_{12}$(SbF_6)$_7$[18] etc. have shown that the main relaxation mechanisms are (1) dipolar interaction between electron and nucleus, dipolar interaction between homo nuclear spins and hetero nuclear spins, other than the contact term and hetero nuclear spins, (2) interaction of the nuclei with conduction electrons (mobile paramagnetic centers), and with the localized, fixed paramagnetic centers.

In this work, T_1^{-1} measurements over a wide range of T and **B** in poly 3-methylthiophene (p3MT) doped with hexafluoro-phosphate (PF_6) are reported, along with measurements of conductivity, σ (B = 0, 77 K < T < 300 K) and the magnetic susceptibility (χ, **B** = 0.1 Tesla, 3.5 K < T < 350 K). The doping level has been varied to tune the conductivity values: in fully doped sample(p3MT-1)σ~ 120 S/cm and in dedoped sample (p3MT-2)σ ~ 5 S/cm; and this facilitates to investigate the role of carrier density and EEI in the NMR relaxation mechanisms. A correlation between electrical conductivity, magnetic susceptibility and relaxation mechanisms has been observed in these samples. The results are analyzed using the modified Korringa relation in the appropriate temperature region, and the deviations are found to be more significant in the less conducting sample. Moreover, it has been observed that the proton spin lattice relaxation data give insight into the dimensionality of the sample and hence with the support of ^{19}F-T_1, the corresponding role of both inter-chain and intra-chain diffusion mechanisms has been suggested.

2. EXPERIMENTAL DETAILS

Conducting p3MT films, doped with PF_6, are prepared by low temperature electrochemical polymerization at – 30 ^{o}C[19]. A 50 mM stoichiometric solution of monomer (3-methyl thiophene), salt (tetrabutylammoniumhexafluorophosphate, $TBAPF_6$) and solvent (propylene carbonate) is made. A cylindrical cell containing highly polished glassy carbon (GC) [used as working/ cathode] and stainless steel [used as counter/anode] electrodes is used to carry out the polymerization. The two electrodes are separated approximately by 6 mm. Before the reaction starts, the solution is ultrasonicated for about 3 min and then was bubbled for about 30 min vigorously by N_2 gas to drive away traces of oxygen from the solution. An inert atmosphere is maintained during the experiment. A

constant current of 1mA/cm^2 for 30 minutes is applied to the electrodes. A free standing film of 45 mm by 45 mm having thickness of 45 μm is formed on the GC electrode at the end of the experiment. A part of the film is peeled off for analysis (considered as highly doped, named = p3MT-1). In the remaining part of the sample (lightly doped named p3MT-2), a reversed current of 0.5 mA/m^2 is applied for 20 minutes to the electrodes. This process of applying reverse current is called de-doping. During the reversed current the PF_6 ions is removed from the prepared polymer system. Both the highly doped (p3MT-1) and lightly doped (p3MT-2) samples are used for conductivity, susceptibility and NMR studies. Since the dopants are intercalated between the polymer chains, the structure of the p3MT chains with dopants looks as depicted in the schematic diagram in Fig. 1[20].

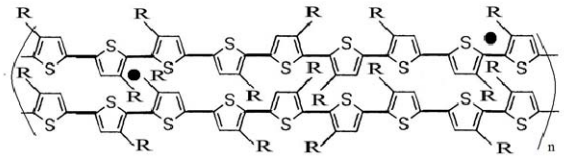

Fig. 1: Schematic diagram of the p3MT polymer with the dopants. Where R = CH_3, methyl side group attached to thiophene ring and•= PF_6 is dopant.

Measurements of σ as a function of T were made using the standard four probe technique using dip stick. The variation of σ as a function of T for p3MT-1 and p3MT-2 are shown in Fig. 2.

Magnetic susceptibility measurements are carried out using Quantum Design SQUID magnetometer between 3.5 K and 350 K at 0.1 T. SQUID measurements of χ for p3MT-1 and p3MT-2as a function of T (3.5 - 350K), are shown in Fig. 3. Since the conductivity of p3MT-2 sample goes down by nearly two orders of magnitude, from 300 to 77 K, it typically shows the activated transport observed in semiconducting systems, so the relaxation studies are carried out only in a limited range of temperature and magnetic field. Meanwhile the charge carrier density in p3MT-1 sample is close to that in metallic systems, as indicated from the magnetic susceptibility data, the detailed high magnetic field ^{1}H-T_1 measurements were done only

in this sample. Measurements of T_1^{-1} as a function of T for ^{1}H and ^{19}F in both samples are shown in Fig. 4. There are two issues involved in the present NMR experiments say measurement of (i) Spin lattice relaxation time and (ii) Doping level in the two samples.

(i) Measurement of spin lattice relaxation time:

Measurements were performed at 0.9T by monitoring the magnetization recovery of the proton spin echo, while measurements at higher fields were conducted by monitoring the recovery of the FID. The ^{1}H measurements in the p3MT-1 sample were done at four values of B (0.9, 9.0, 16.4 and 23.4 T) as shown in Fig. 4a, while the p3MT-2 sample was measured only at 0.9 T. ^{19}F- T_1 measurement at 9.0Tis also doneusing FID signals (Fig. 4b).

(ii) Doping level calculation:

Measurement of the doping level in the two samples has been carried out at 0.9 T, by taking the ratio of the number of ^{19}F spins to that of ^{1}H spins. For this purpose, the experiment has been conducted in the following manner. The number of protons are estimated by first measuring the T_1 of the sample protons by monitoring the recovery of the free induction decay after application of a saturation train to estimate the value of T_1. Another FID was recorded after waiting for an appropriate time interval of (5 times T_1) so as to ensure the complete recovery of the magnetization. Similarly, a T_1 measurement was performed on the Fluorine in each sample; only in the case of Fluorine an echo was monitored to minimize spurious signal contributions. With the recovery time determined, a fully recovered Fluorine FID was recorded. Then, the maximum magnitudes of the recorded FID signals were used to determine the ratio of PF_6 dopants to the single ring monomer units of the polythiophene. The calculation assumed that the receiving coil was identically tuned and matched in the case of the two nuclei, but took into account the relative sensitivity of the nuclei themselves, as well as the number of protons on each ring.This estimation shows that p3MT-1 has a dopant concentration of ~ 0.1 per ring while p3MT-2 has ~ 0.02 per ring (a monomer unit).

3. RESULTS AND DISCUSSION

3.A. Electrical conductivity and magnetic susceptibility

Samples p3MT-1 and p3MT-2 have room temperature conductivities of 120 S/cm and 5 S/cm respectively. A plot of lnσ as a function of 1/T for p3MT-1[σ(300 K) ~ 120 S/cm)] and p3MT-2[σ(300 K) ~ 5 S/cm)] shown in Fig. 2 which shows a semiconducting behavior. The data at T < 70 K (not shown) show some scattering due to the increase in the contact resistance at lower temperatures. The fit shows a linear behavior for both the samples indicating a thermally activated transport.From the Arrhenius plot it is observed that activation energies of p3MT-1 and p3MT-2 samples are 21.7 meV and 24.7 meV which are above the minimum level (~ 10 meV) of thermal activation process. Moreover,both the samples are doped and thus have high charge carrier concentration of the order of 10^{20} which in turn decreases the hopping length. Thus it helps in enhancing hopping transport process. Although σ(300 K) for p3MT-1 has the same order of magnitude as that for

metallic polypyrrole (PPy) and polyaniline[21], its (σ) strong reduction with decreasing temperature suggests that a large number of carriers undergo intra-chain localization at low temperature. This behavior was further investigated using measurements of susceptibility.

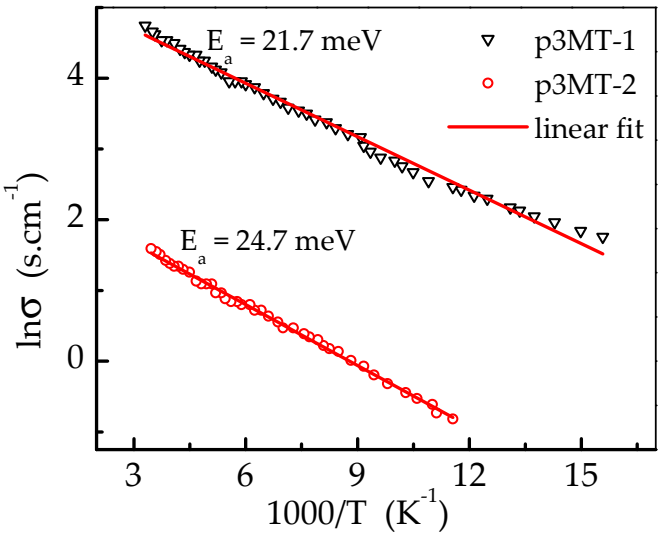

Fig. 2: Temperature (T) dependence of conductivity (σ) for p3MT-1 (∇) and p3MT-2 (O).

The susceptibility χ(T) for p3MT-1 and p3MT-2 as a function of T_1^{-1} at 0.1 T is shown in Fig.3. Results of susceptibility vs temperature of the samples display a Fermi Glass behavior[22], which is characterized by the existence of Pauli susceptibility at high temperatures, with a Curie contribution to susceptibility appearing at lower temperatures.

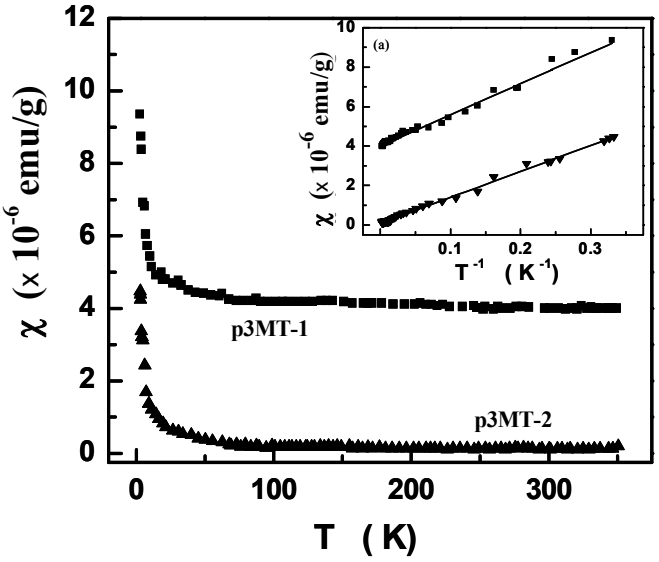

Fig. 3: Temperature dependence of Susceptibility for p3MT-1 (■) and p3MT-2 (▲) at 0.1 T. Inset: Susceptibility as a function of T^{-1}, Solid line is fit to the Eq. (1).

A good fit to the data is obtained by using a sum of Curie and Pauli susceptibility,

$$\chi = \chi_c + \chi_P \qquad (1)$$

where $\chi_c = N_c \mu_B^2 / k_B T$ and $\chi_P = \mu_B^2 N(E_F)$ are respectively the Curie and Pauli susceptibilities, N_c is the number of Curie spins, k_B is the Boltzmann constant, $N(E_F)$ is the conduction electron density of states at Fermi energy (E_F) and μ_B is the Bohr magneton. This behavior is widely observed in several conducting polymers due to the coexistence of both Curie and Pauli spins, since the carriers tend to be localized in the amorphous regions and are delocalized in the partially crystalline domains[22-27]. The fit parameters obtained from these data are listed in Table I.

Table I. Parameters for σ and χ_P, $N(E_F)$ and N for p3MT-1 and p3MT-2. The susceptibility parameters are obtained from the fit to Eq. (1).

Sample	σ (~300 K) (S/cm)	χ_P (emu/gm)	$N(E_F)$ (states/eV – C)	N_c (per ring)
p3MT-1	120	4×10^{-6}	1.48	3.15×10^{13}
p3MT-2	5	0.85×10^{-7}	0.03	2.07×10^{13}

The Pauli contribution provides a direct measure of N(E_F), indicating that the number of delocalized carriers in p3MT-1 is rather high. The value of N(E_F) in p3MT-1 is ~50 times larger than that of p3MT-2, while the number of Curie spins is nearly the same in both samples. These results agree with the larger value of σ (24 times larger) observed in p3MT-1. In p3MT-1, the Curie and Pauli terms are equal at around 4.2 K. These values of χ_P and N(E_F) are comparable with the earlier reports in conducting polymers[28]. Thus we have seen that there is consistency between the conductivity of the samples, doping level and N(E_F).

3.B. Presentation of the ^{1}H and ^{19}F NMR T_1 data

In this Section, we describe the important features of the ^{1}H-T_1 and ^{19}F-T_1- data as a function of the Larmor frequency (f) and temperature as shown in Figures 4a and 4b.

1. T_1^{-1} shows a substantial dependence on both frequency and temperature, which is quite different from those observed in normal metals like Cu, etc[1].

2. As seen in Fig. 4a, T_1^{-1} at 0.9T has a maximum at T below 200 K that occurs at 182 K and 165 K, respectively for p3MT-1 and p3MT-2. Since this feature is more pronounced in the former, more detailed studies are carried out for p3MT-1 at higher magnetic fields. The data in Fig.4a also show that this maximum is smeared out and shifted to higher temperature at 16.4 T and 23.4 T.

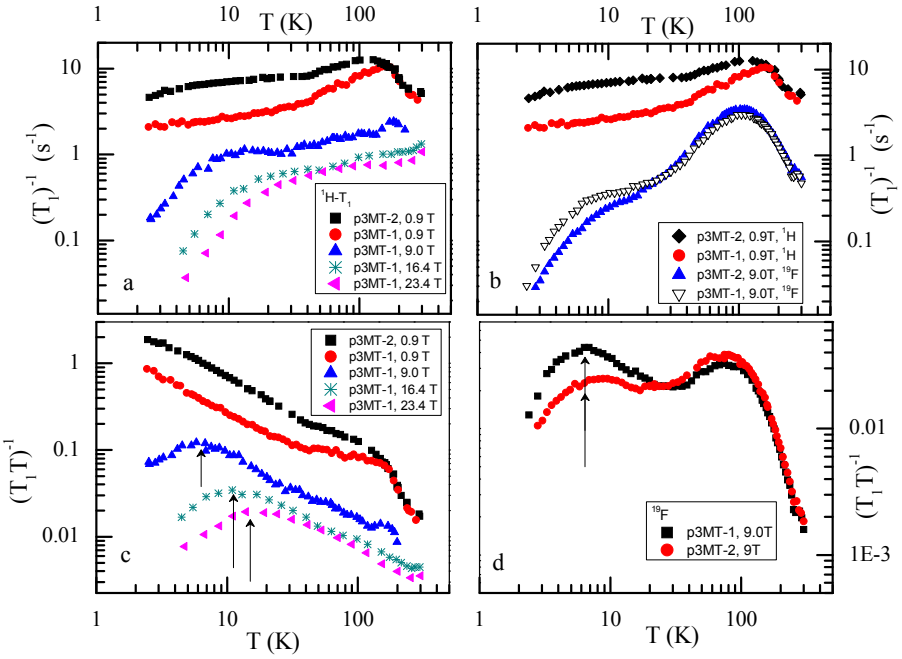

Fig. 4: (a) ^{1}H $1/T_1$ as a function of T for p3MT-2 at 0.9T and p3MT- 1 at 0.9, 9.0, 16.4, and 23.4 T. (b) Plot of ^{19}F- T_1^{-1} as a function of T for p3MT- 2 (▲) and p3MT-1 (∇) at 9 T and comparison to ^{1}H-T_1^{-1} for p3MT-2 (■) and p3MT-1 (●) at 0.9 T. (c) ^{1}H-$(T_1T)^{-1}$ as a function of T for p3MT-2 at 0.9T and p3MT-1 at 0.9, 9.0, 16.4, and 23.4 T.(d) Plot of ^{19}F-$(T_1T)^{-1}$ as a

function of T for p3MT-2(•)and p3MT-1(■)at 9 T. The vertical arrows show the value of T given by the condition $g\mu_B B = 2k_B T$.

3.The ^{19}F-T_1^{-1} data for both samples at 9.0 T in Fig. 4b show a maximum at around 100 K. This value of temperature is significantly lower than the temperature, where ^{1}H-T_1^{-1} maximum was observed at 9.0 T (~182 K) in Fig. 4a.
4.Another important feature of Fig. 4 is that at 0.9 T, T_1^{-1} for ^{1}H below 150 K is less for p3MT-1 than for p3MT-2.
5.Unlike ^{1}H-T_1, ^{19}F relaxation rate (Fig. 4b) show a crossover in relaxation rate between these two samples at T ~ 25 K; i.e., T_1^{-1} for^{19}F in p3MT-1 is larger than in p3MT-2 below 25K.
6.To emphasize the deviation from Korringa behavior, we are plotting $(T_1T)^{-1}$ vs. T as shown in Fig.4c and Fig. 4d. The 0.9 T data shows a negative slope in $(T_1T)^{-1}$ vs T plot with increasing temperature while the same sample at 9.0T, 16.4 T and 23.4 T similar trends is observed from 8 – 120 K, 15 – 250 K and 20 – 250 K respectively.While at lower temperature there is the drop in $(T_1T)^{-1}$ with decreasing temperature that occurs near 6.04 K for 9.0 **T**, 11.02 K for 16.4 **T**, and 15.72 K for 23.4**T**

Fig.4d shows $(T_1T)^{-1}$ as a function of temperature for ^{19}F in both samples at 9.0 **T**. ^{19}F-$(T_1T)^{-1}$ has two broad peaks, one around 110 K for both samples (in the form of thesuperposition of two peaks) and other peaks at 6.5 K and 8.0 K for p3MT-1 and p3MT-2 respectively. An interpretation of these results is presented in Section C.2.1.b.
The salient features in relaxation times are (i) change of slope in$(T_1T)^{-1}$ with T at temperature$T_z = \frac{g\mu_B \boldsymbol{B}}{2k_B}$and (ii) the observation of a crossover of T_1 in ^{19}F.

3.C. Analysis of NMR T_1

The observed NMR-T_1 data for both the samples, has substantial dependence not only on temperature and Larmor frequency, but also depend on the sample conductivity. It might obviously due to the disorder nature of conducting polymers resulting in a wide range of electron dynamics and interactions at different values of temperature, frequency and conductivity. To get a better insight, one can analyze the T_1data by considering its variation with respect to-(1) frequency (2) temperature and (3) the NMR nuclei under study.

C.1: Analysis of T_1 as a function of frequency.

Before analyzing the T_1^{-1} against temperature data, in the present system, it is important to find out the dimensionality of the system under consideration. There are many studies[14-17, 29-31] where NMR relaxation rate as a function of Larmor frequency in systems like conducting polymer and organic salts have been reported. They also reported that plot of T_1^{-1} against frequency gives the information about the dimensionality of the

system. It has been shown that the spectral density function, f(ω), reflects the electronic spin motion and depends sensitively on the dimensionality of the process. In one dimension,f(ω) is proportional to $\omega^{-1/2}$ and in two dimensions f(ω) displays a logarithmic divergence, while in three dimensions, it is nearly constant.

It is found that in majority of the T_1 studies in conducting polymers and organic salts have been carried out either at low frequency as a function of temperature or high frequencies at room temperature only. Thus it is evident that a system can show different dimensionality depending upon the selection of temperature and frequency. Hence, with these limited experiments covered in the literature, it is difficult to draw a converging conclusion on the system dimensionality.

We have carried out frequency dependence of T_1^{-1} in p3MET-1. Fig.5 shows T_1^{-1} vs frequency($f = \omega/2\pi$) for a few representative temperatures. The frequency dependence of T_1^{-1} does not follow similar pattern for all the temperatures studied. Dimensionality dependence of the system can also be classified from the nature of the frequency dependence of T_1^{-1} data. In the case of 3-D, T_1^{-1} is independent of frequency while T_1^{-1} is logarithmic dependence of frequency for 2-D. However, for q1-D, T_1^{-1} follows $f^{-1/2}$.

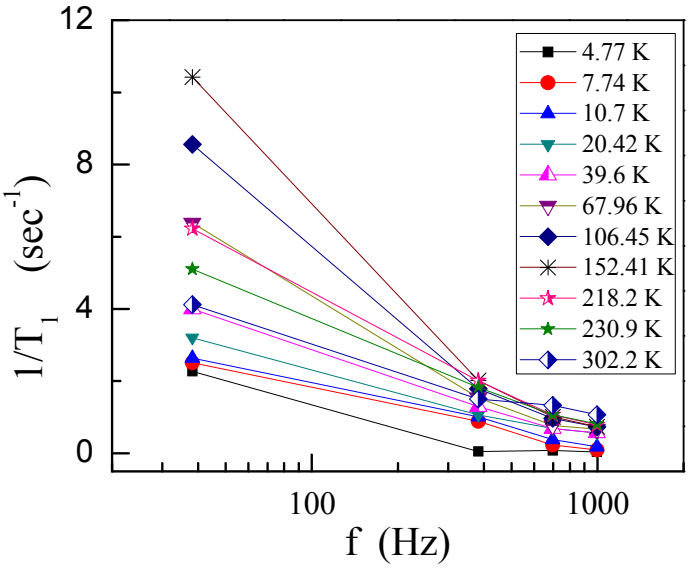

Fig.5a. ^{1}H-$T_1$for p3MT-1 as a function of frequency for a few representative temperatures. Solid line is guide to the eye.

For the lowest temperature studied, 4.77K, T_1^{-1} is independent of frequency except in the case of Larmor frequency 38.3 MHz (Fig. 5a). The orientational degrees of freedom of localized electrons are producing a fluctuating field which has Fourier components at Larmor frequency. Below Zeeman splitting temperature ($T_Z = \frac{g\mu_B B}{2k_B}$) at a given field, these orientational degrees of freedom cease to exist. Thus, for a field, below its Zeeman

splitting temperature the spin diffusion to paramagnetic centers freezes out. In other words, conduction electrons are pinned by the applied magnetic field below its Zeeman splitting temperature. The corresponding Zeeman splitting temperature for conduction electrons in the magnetic fields 0.9 **T,** 9.0 **T,** 16.4 **T,**and 23.4 **T** below which the conduction electrons are pinned are 0.6 K, 6.04 K, 11.02 K and 15.72 K respectively. This is consistent with experimental data (shown in Fig.5a). 4.77 K satisfies the condition $T < T_Z$ for the frequencies corresponding to the field 9.0 **T**, 16.4 **T** and 23.4 **T** but not for 0.9 **T.** This explains the deviation of T_1 for 38.3 MHz at 4.77 K. This independent behavior of T_1^{-1} with frequency suggest that the system behaves as 3-D below temperatures, $T < T_Z$.

We also analyzed the T_1^{-1} vs f data with respect to temperature greater than T_Z to find the dimensionality of the system. Fig. 5b and 5c shows that the representative fit to the 2-D model (T_1^{-1} logarithmic divergence of f) and q1-D model ($f^{-1/2}$ dependence of T_1^{-1}) respectively. To identify the correct dimensionality, we have plotted the R^2 for the least square fit for 2-D and q1-D in the Fig. 5d. From the figure it is observed that higher the temperature better is the q1-D model compared to the 2-D model. From the analysis at 302.2 K, where T_1^{-1} follows best fit to $f^{-0.5}$, it is observed that the diffusion constant, D = 1.48 x 10^{-10} cm^2s^{-1}.

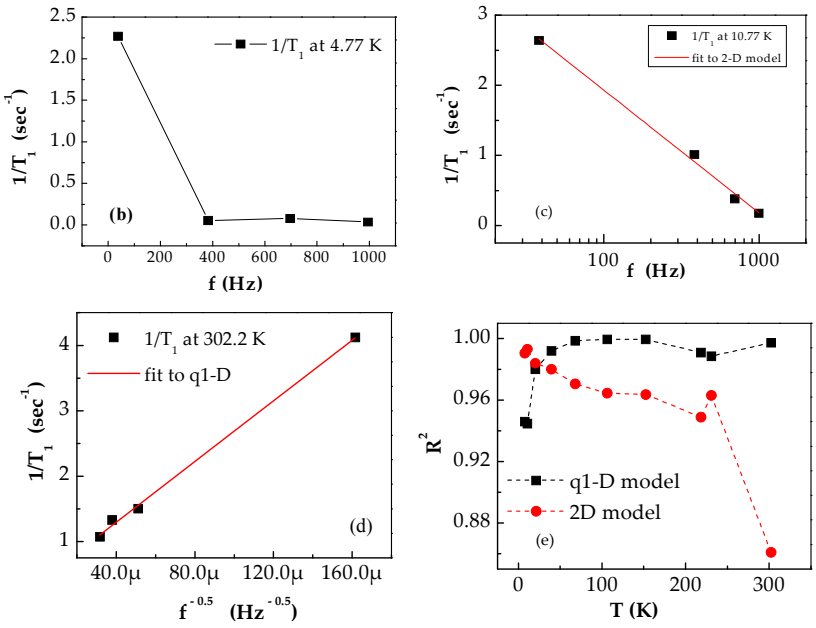

Fig.5b. ^{1}H-T_1 as a function of frequency at 4.77 K. Solid line is guide to the eye. (c). ^{1}H-T_1 as a function of frequency at 10.7 K. Solid line is Fit to the 2-D model. (d). ^{1}H-T_1 as a function of frequency at 302.2 K. Solid line is Fit to the q1-D model. (e). R^2 for the fit to the models q1-D and 2-D as a function of temperature. Dash lines are just guide to the eye.

Our analysis in the present system shows that, at temperatures below T_Z, system shows 3-D behavior, while as the temperature increases the dimensionality changes over to 2-Dand then to q1-D. This indicates that the dimensionality of the system depends on the selection of frequency and temperature, as observed in earlier studies [14,30] .

C.2. Temperature dependence of Relaxation rate:

We consider the following relaxation mechanisms to explain the observed T_1Vs temperature behavior.(1) Dipolar interaction between homo and hetero nuclei modulated by the re-orientation motion of the symmetric sub-groups, (2) Spin Diffusion to Paramagnetic Centers (SDPC) and (3) relaxation by the translational and spin motion of the conduction electrons. The relative magnitude of each of these mechanisms to T_1^{-1} will depend on the range of temperature. When the conduction electrons are hopping between the localization sites, both their spin orientation and translational motion can contribute to T_1^{-1}. But when we consider free conduction band electrons, only the translational motion is important for T_1^{-1}, and a Korringa type of relaxation is expected. Thus, for the sake of convenience, the T_1 analysis has been carried out in three different temperature regions where the relaxation is dominated by (a) modified BPP type relaxation[32], (b) the SDPC along with modified Korringa relaxation and (c) the 'modified Korringa like' relaxation.

In the p3MT-1 system, as different types of T_1^{-1} variation with respect to temperature is observed, we are forced to consider different types of possible NMR relaxation mechanisms depending on the temperature range. The variation in T_1^{-1} against temperature is more pronounced at low Larmor frequency (0.9T) than higher frequencies (9.0 T, 16.4 T, and 23.4 T),which is in concurrence with the observations of Nechtschein et.al.[14] and Mizoguchi et.al.[15,30] that the same material behaves like quasi 1-D at high frequencies and deviates to 3-D behaviour at low frequencies. This is because of the spectral density due to reorientation motion of the symmetric molecular groups having finite Fourier components at lower fields than at high fields.

Thus for more detailed study, we shall consider the data at low frequency, 0.9T, which is presented in 2 and 4 of section 3.B. The observation of T_1^{-1} maximum at high temperature may due to the reorientation motion of the symmetric groups like CH_3 and PF_6 present in the system and thus following the modified BPP model.Thus it is acceptable to expect a BPP type relaxation mechanism to interpret the T_1^{-1} maximum at high temperature for 0.9T, asit gives more insight in to the physics of the system.

C.2.1. Relaxation mechanism due to reorientation motions of symmetric groups

(a) ^{1}H-T_1 Studies:

The variation of ^{1}H-T_1 at T above 50 K is shown in Fig. 6afor low field (0.9 T) data for both samples and high field (9 T) data for p3MT-1 is in Fig. 6b. The data for each sample in Fig. 6a show a broad maximum due to the activated motion of the reorientation of methyl groups. As mentioned earlier, the ^{1}H-T_1 behavior at T above 50 K is analyzed by considering the magnetic dipolar interactions among proton–proton and proton–fluorine that are modulated by the reorientational motion of symmetric groups such as CH_3 and PF_6. Initially, the T_1 data analysis has been tried with this model by assuming only one type of CH_3 group, and the fit was not satisfactory. Since the system is a disordered one, all

of the CH_3 groups may not at an energetically equivalent environment. In the next step, the same model has been tried by considering two inequivalent CH_3 groups: (i) CH_3 groups close to PF_6, (i.e. CH_3-1) and (ii) CH_3 groups away from PF_6, (i.e. CH_3-2)with their corresponding activation energies (E_{HH1} and E_{HH2}) and correlation times (τ_{HH1} and τ_{HH2}), along with a common correlation times (τ_{HF}) for ^1H and ^{19}F cross relaxation with an activation energy (E_{HF}) for PF_6 reorientation. The corresponding rate equation for the modified BPP model is given by[13, 30, 32-35]:

$$\frac{1}{T_{1H}} = C_{HH1}\left(J(\tau_{HH1},\omega_{HH1}) + 4J(\tau_{HH1},2\omega_{HH1})\right) + C_{HH2}\left(J(\tau_{HH2},\omega_{HH2}) + 2J(\tau_{HH2},2\omega_{HH2})\right)$$
$$+ C_{HF}\left(J(\tau_{HF},(\omega_H - \omega_F)) + 3J(\tau_{HF},\omega_H) + 6J(\tau_{HF},(\omega_H + \omega_F)\right) \qquad (2)$$

where C′s are interaction constant, $J(\tau_{i,}\omega_N) = \frac{\tau_i}{1+(\omega_N\tau_i)^2}$ and correlation time τ_i: $\tau_i = \tau_{i0}e^{\frac{E_i}{k_BT}}$. The least square fit has been carried out by using MATLAB.

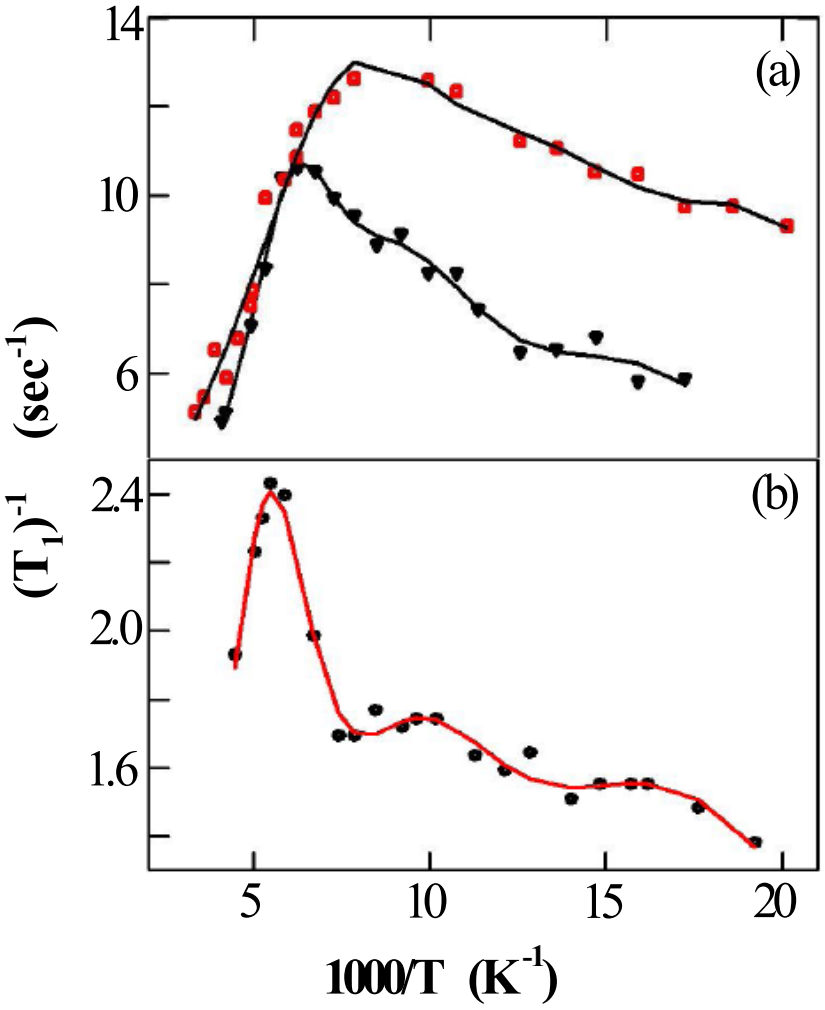

Fig. 6. BPP model fit to (a) ^{1}H $1/T_1$ as a function of T for p3MT-1 (▼) and p3MT-2 (◘) at 0.9T
(b) p3MT-1 (•) at 9 T. The solid lines are a fit to Eq. 2.

The motional parameters from the best fit to the modified BPP model for ^{1}H-T_1 is compiled in Table II.The motion induced relaxation mechanism of the ^{1}H nuclei can be inferred from the shift of the position of the T_1^{-1} maximum to higher temperature at a Larmor frequency of 383 MHz compared to the position at 38.3 MHz. The predicted curve for 9.0T ^{1}H- T_1^{-1} by using the fit parameters of 0.9T ^{1}H-T_1^{-1} for p3MET-1 gives the similar features with the measured parameters, which is a sign of consistent description by the BPP model. However the measured relaxation ^{1}H-T_1^{-1} data is almost a factor of 1.3 higher than the predicted data by the fit parameters obtained at 38.3 MHz. This deviation from the BPP model hints that,with increasing Larmor frequency, the contribution of the re-orientational motion to the intensity of the spectral density function decreases.Nevertheless the position of the maximum can be correctly predicted by the modified BPP model which gives the credit to the relevant fit parameters.

Table II. Fit parameters fit to Eq. (2).

Parameters	P3MT-1			P3MT-2	
	^{19}F (9.0 T)	^{1}H (9.0 T)	^{1}H (0.9 T)	^{19}F (9.0 T)	^{1}H (0.9 T)
τ_{ii01} (x 10^{-12} sec)	1.63	0.18	0.639	7.54	1.38
τ_{ii02} (x 10^{-11} sec)	4.71	14.2	34.3	0.406	6.01
τ_{ij0} (x 10^{-11} sec)	1.53	0.213	18.54	1.06	0.752
E_{ii1} (meV)	62.49	80.28	84.62	23.43	32.98
E_{ii2} (meV)	33.416	23.82	40.967	44.967	21.525
E_{ij} (meV)	26.038	27.51	19.529	24.389	42.92
K_{ii1}(x 10^9 sec^{-2})	1.94	2.68	0.992	3.55	1.69
K_{ii2}(x 10^9 sec^{-2})	3.66	2.15	0.937	3.08	1.269
K_{ij} (x 10^8 sec^{-2})	11.16	3.2	1.59	3.15	1.346
τ_{ii1} (x 10^{-10} sec)*	22.7	19.89	116.8	1.147	0.632
τ_{ii2} (x 10^{-9} sec)*	2.26	2.25	39.6	0.724	0.729
τ_{ij} (x 10^{-10} sec)*	3.13	0.517	17.8	1.79	6.9

*τ_{ij} and τ_{iin} are calculated at 100 K, using the relation $\tau_{iin} = \tau_{iio} \times e^{E_{iin}/k_B T}$. Subscript i and j are the NMR nuclei.

Our observation above, at lower frequencies show a reorientational motion of the CH_3 groups which is unnoticed at higher Larmor frequencies is similar to the ones studied by Mizoguchiet.al.[30] who have carried out experiments of T_1^{-1} versus temperature as well as frequency dependence studies in FSO_3 doped PA (10^5 S/cm). They have done the experiments at considerably low NMR frequencies and over a wide temperature range. Their T_1 analysis with frequency shows quasi-1d behavior at high frequencies and at low temperatures, while the fit deviates at lower frequencies and high temperatures. These results also suggest that at high temperature and low frequency, the sample behave slike a 3-d system. They interpreted, the observed T_1^{-1} maximum at high temperature regionmay be due to molecular motion of FSO_3 groups, the residual moisture and, or other reorienting groups.

Nechtschein et.al.[14] have also shown the frequency dependence of T_1 in doped and undoped polyacetylene (PA). They observed the q1-D nature in both the PAs throughout the temperature range of study, except at very low temperatures. They also concluded that at low frequency, the 1-D diffusion breaks down because of inter-chain hopping and 2-D or 3-D behavior is expected. The cross over between 1-D and 2-D (or 3-D) regimes is expected to occur when the inter-chain hopping frequency is of the same order of magnitude as the Larmor frequency. Their analysis further showed that the intra chain diffusion follows power law behavior, T^n (n=0.65 above 50 K and n=1.5 below 50 K). Similar trend of change of dimensionality has been noticed by Sachs et.al.[29] Their ^{1}H-T_1 studies at 293K, in organic conductors $(FA)_2PF_6$ shows the relaxation is an evidence of 1-D diffusive motion. At low frequency the 1-d model diverges.They concluded that lattice imperfections are known to spoil the one-dimensionality of the sample.

(b) ^{19}F-T_1 Studies:

Fig.7 shows T_1^{-1} for ^{19}F at 9.0 T as a function of T above 40 K for p3MT-1 and p3MT-2. The main sources for the ^{19}F relaxation are the fluctuating magnetic fields associated with the rotational motion of the PF_6 groups. Because the hyperfine field of the conduction electrons at the ^{19}F sites is expected to be weak and this contribution will not be considered further. In detail, the relaxation mechanisms for ^{19}F are: (i) the ^{19}F-^{19}F interaction, within the same PF_6 groups, (ii) the ^{19}F-^{19}F interactions between different PF_6 groups, (iii) the magnetic dipole interaction between ^{19}F and ^{1}H nuclei, (iv) the magnetic dipole interaction between the ^{19}F and ^{31}P nuclei and (v) contribution from chemical shield anisotropy (CSA) of PF_6. Since the interaction constants are inversely proportional to r^6 (where r is the inter-nuclear distance) and different PF_6 groups are well separated, the contribution to T_1 from the ^{19}F-^{19}F interactions between different PF_6 groups is small enough and this term is left out in the following analysis. Also, because the ratio of the Larmor frequencies of ^{31}P to ^{19}F is ~ 0.432, the ^{31}P to ^{19}F cross relaxation is not expected to play a significant role in the ^{19}F relaxation process[36].

An estimate of the contribution to T_1 from chemical shield anisotropy (CSA, $\Delta\sigma$) of PF_6 groups is carried out. In samples containing fluorine nuclei, CSA may contribute to the relaxation depending on whether PF_6 is acting as a counter ion strongly or weakly interacting with the polymer chains. The ^{19}F line width normalized absorption spectra for both samples p3MT-1 and p3MT-2 at various temperatures (figure not shown) have been used to estimate the Full Width at Half Maximum (FWHM). FWHM for both samples p3MT-1 and p3MT-2 varies from 30 kHz at 250 K to a maximum of 70 kHz at 2.78 K.Our T_1 analysis including CSA contribution (along with reorientational motion of symmetric groups) to relaxation mechanism shows a pre-exponential factor (τ_{CSA0}) = 1.35 x 10^{-9} sec and activation energy (E_{CSA}) = 146 meV. The corresponding CSA ($\Delta\sigma$) is $\Delta\sigma$ = 225 ppm which is comparable to the reported values in similar systems. With these fit parameter values, CSA contribution (at 250 K) to T_{1total}^{-1}; is about 10^{-6} s^{-1}, which is quite small compared to the contribution from dipolar interactionmodulated by the reorientational mechanism. Hence ^{19}F CSA contribution has not been considered for ^{19}F, T_1^{-1} analysis.

On the other hand, the Larmor frequency of hydrogen nuclei is 1.063 times higher than that of fluorine nuclei. This shows that the cross relaxation between fluorine and hydrogen nuclei also plays a prominent role in T_1^{-1} for ^{19}F at T above 40 K. Thus the ^{19}F relaxation mechanisms are mainly due to the magnetic dipole-dipole interactions modulated by: (i) the random reorientations of PF_6 and (ii) isotropic reorientations of CH_3 groups. Under these circumstances, T_1^{-1} for ^{19}F will follow the same modified BPP model described by Eq. (2), where the subscript H changes to F and F changes to H.

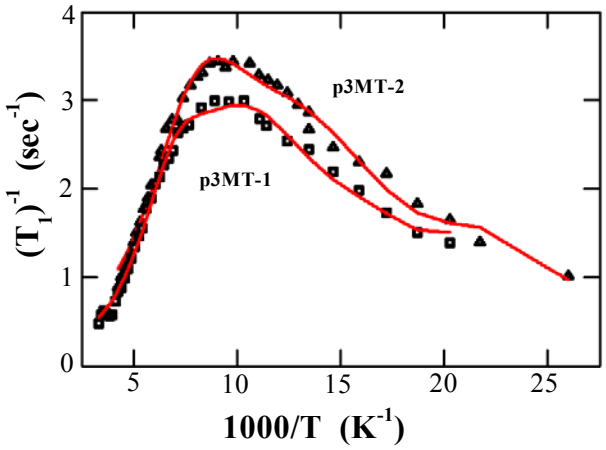

Fig. 7: BPP model fit to^{19}F $1/T_1$ as a function of T for p3MT-1 (◘) and p3MT-2 (▲) at 9.0 T. The solid lines are a fit to Eq. 2.

The motional parameters from the best fit to the modified BPP model, for both ^{19}F-T_1 and ^{1}H-T_1, are compiled in Table II. The analysis of ^{19}F and ^{1}H relaxation data obtained using this model suggests the following: Since PF_6 is relatively free to reorient, the maxima is shifted to lower temperatures, and also it is broader due to the role of inter-chain

disorder in the relaxation mechanism. Furthermore, the relaxation data for ^{19}F in both samples are nearly identical due to the less dominant role played by the conduction electrons among these samples, and the extent of inter-chain disorder is rather similar in both systems.

It is revealed from the above two analysis that even though PF_6 is a heavier group than CH_3, the T_1^{-1} maximum at 9.0 T in case of ^{19}F is observed at lower temperature compared to ^1H at that field. This can be explained by considering the fact that, the PF_6 group is relatively free to reorient as it is situated in between the chains (see Fig. 1) whereas CH_3 is attached to the polymer backbone. Thus the correlation time for PF_6 is shorter than that of CH_3, accordingly the T_1^{-1} maximum for PF_6 motion is observed at lower temperatures. It is evident from the general BPP equation that T_1 exhibits a minimum when $\omega_0\tau_c = 0.615$, and the corresponding maximum in T_1^{-1} of nuclei 'i' with nuclear spin I is given by $T_{1i}^{-1} = \frac{3\times1.42\gamma_i^4\hbar^2 I(I+1)}{2r^6\omega_{oi}}$, where γ_i is the nuclear gyromagnetic ratio of nuclei i, ħ is the reduced Planck's constant, r is the inter nuclei distances and ω_{oi} is the Larmor frequency of the nuclei i. It has been found that $T_{1H}^{-1}/T_{1F}^{-1} > 1$, from the known values of γ, ω_o, r, I and ħ for ^{19}F and ^1H. This has been further verified from the estimated values of $\omega_{0H}\tau_{cHH}$ and $\omega_{0F}\tau_{cFF}$ at a given temperature (say *150* K), and found that τ_{cFF} being shorter than τ_{cHH} due to the facile motion of PF_6, as explained above.

Similar observation of PF_6 motion has been studied by Wieland et.al.[31] in organic metal $(PERYLENE)_2(AsF_6)_{0.75}(PF_6)_{0.35}x\ 0.85CH_2Cl_2$. Their ^1H-T_1 studies revealed a linear dependence of T_1^{-1} against $f^{-1/2}$, showing a signature of a one-dimensional motion of the spins. T_1^{-1} against temperature in the range 300 to 180K, showed a linear variation as expected of a organic metal. Observed T_1^{-1} maximum around 50K, is ascribed to theircoupling to the ^{19}F spins of reorienting PF_6 groups. This also supports the view that ^1H relaxation shows signatures of relaxation due to one dimensional motion of spins as well as reorienting groups depending on which process dominates at the temperature under consideration. Hoptneret.al.[17] have carried out ^1H-T_1 and ^{19}F-T_1in radical cation salt, $(fluoranthenyl)_2^+PF_6^-$as a function of temperature. They observed that ^{19}F-T_1 are relaxed mainly by the reorientational motion of the anions and by the interaction with fixed paramagnetic impurities, the protons are relaxed additionally above 150 K predominantly by highly mobile paramagnetic species, whose concentration could be determined directly via the NMR signal amplitude. These observations support our view of PF_6 reorientation motion responsible for spin lattice relaxation. Korringa relation observed for proton relaxation shows that it is metallic above 183K. Further, frequency dependence of T_1ofproton relaxation supports the one-dimensional spin transport and also confirms that only protons of the cation stacks are relaxed by the highly mobile paramagnetic species.

C.2.2: Relaxation mechanism dominated by Spin Diffusion to Paramagnetic Centres (SDPC) and the modified Korringa relation

As the temperature decreases, the relaxation due to the reorientation motions of the symmetric groups slows down and freezes at a particular temperature. Once temperature is low enough, the main contribution to the relaxation mechanism is due to the SDPC process and the motion of charge carriers.A cartoon of the SDPC process is shown in Fig. 8, where the filled black circle is the paramagnetic center, the elliptical shaped one's are the nuclear spins, the nuclei inside the shaded region are shifted in frequency so much that they donot interact with the others, the nuclei within the radii **d** and **b**are relaxeddirectly by the fluctuating magnetic field generated by exchanging magnetization to the paramagnetic center (frozen electrons), and those outside the radius b are relaxed by nuclear spin diffusion. In the spin diffusion process, the spins closer to the paramagnetic center recover more quickly than those farther away.But after a long enough time, all of them reach an equilibrium spin temperature. These types of relaxation mechanisms have been reported in other systems[1,37-39].

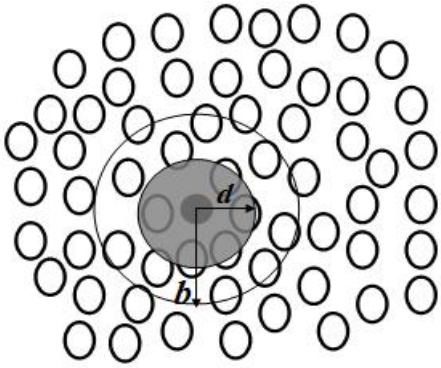

Fig.8. Cartoon of the SDPC process. • = paramagnetic center.0 = nuclear spins.**d** region = region of frequency shifted nuclei. **b**– **d**= region of nuclei that directly relaxed to paramagnetic centre. Nuclei outside the region**b** are relaxed by nuclear spin diffusion.

It is interesting to recall that as the temperature decreases, T_1 behavior is more and more towards 3-D. Since the protons are in the polymer back bone and thus their relaxation may be mainly due to both intra- and inter chain hopping of the charge carriers.

At temperatures below 50 K, T_1^{-1} is proportional to temperature as shown in Fig. 9. This follows the modified Korringa relation, as reported earlier in PPy-PF_6. The analysis of T_1 data using the modified Korringa relation[11, 40] takes into account of the contributions due to disorder and EEI[3,12, 17, 41-45] is expressed as[3, 13, 17, 45]

$$K^2 T_1 T\left(1+\frac{\varepsilon}{2}\right)C_o S_K = 1 \qquad (3)$$

Here $C_0 = (\gamma_n/\gamma_e)^2(4\pi k_B/\hbar)$, ε (= Knight shift anisotropy = d^2/a^2) is the ratio of the anisotropic and isotropic contributions to the hyperfine interaction[3], which plays an important role in the relaxation of organic materials, S_K is the Korringa enhancement factor which includes the role of EEI along with disorder.Korringa enhancement factor contains the spectral density of interaction and is expressed as

$$S_K = \frac{1}{2}\left(\frac{\tau_\perp}{\tau_s}\right)^{1/2}\left[\frac{3}{5}\varepsilon J(\omega_n) + \left(1+\frac{7}{5}\varepsilon\right)J(\omega_e)\right]K_o(\alpha) + \frac{1}{2}(1+2\varepsilon)K_{2k_F}(\alpha) \qquad (4)$$

The quantity ε (= d^2/a^2) is the ratio of anisotropic to isotropic contribution of the hyperfine interaction and $J(\omega) = [(1+\omega^2\tau_\perp^2)^{1/2}+1]/[2(1+\omega^2\tau_\perp^2)]$, is the spectral density of interaction with ω_e and ω_n being the electron and nuclear precession frequencies respectively. In addition to this, $K_o(\alpha)$ and $K_{2kF}(\alpha)$ are given by the expressions: $K_o(\alpha) = (1-\alpha)^{1/2}$ and $K_{2kF}(\alpha) = (1-\alpha)^2/[1-\alpha F(2k_F)]^2$; $F(2k_F) = (1/2)[\ln(4.56T_F/T)]$, the Lindhart function and T_F is the Fermi temperature. In this expression $\tau_\perp$ is the inter-chain hopping time and τ_s is the phonon scattering time along the chain and α is the interaction parameter. For classical metals, ε = 0 and $S_K = 1$, and the Korringa relation is recovered. In organic conductors, for example fluoranthene-PF_6, with highly anisotropic conduction, S_K has values from 50 – 500, and $0 < \varepsilon < 4$, showing a large deviation from that of a classical metal[46].

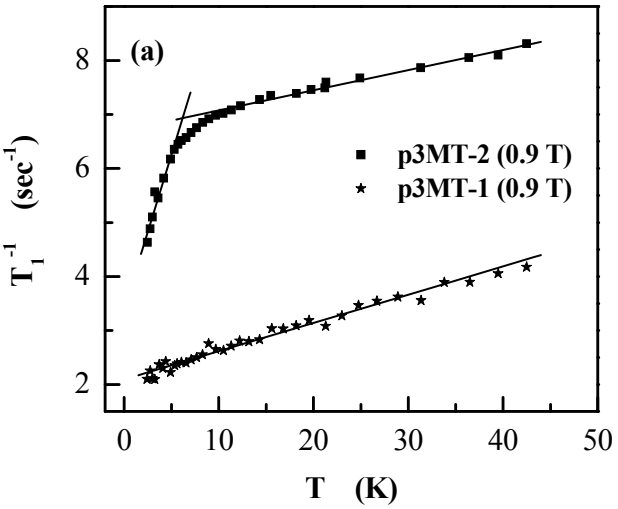

Fig.9a: ^{1}H-T_1 dependence of temperature at 0.9 T. Solid line is fit to the modified Korringa relation expressed by Eq. (3).

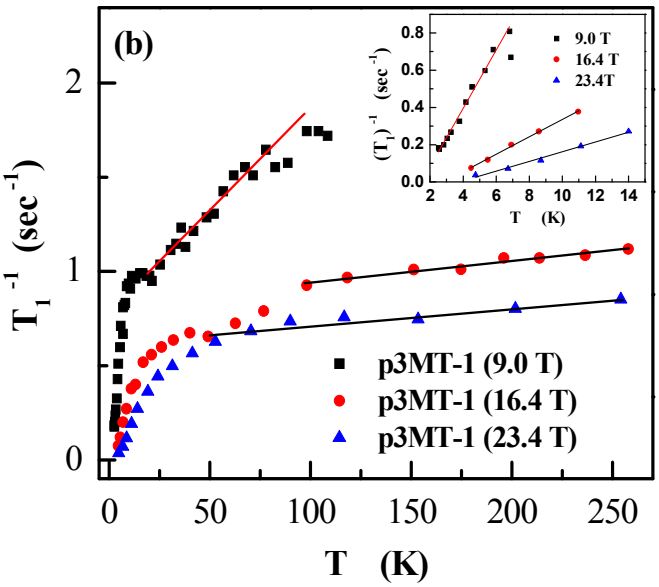

Fig.9b: ^{1}H-T_1 dependence of temperature of p3MT-1 at various fields. Inset: ^{1}H-T_1 as a function of temperature, T < T_Z . Solid line is fit to the modified Korringa relation expressed by Eq. (3).

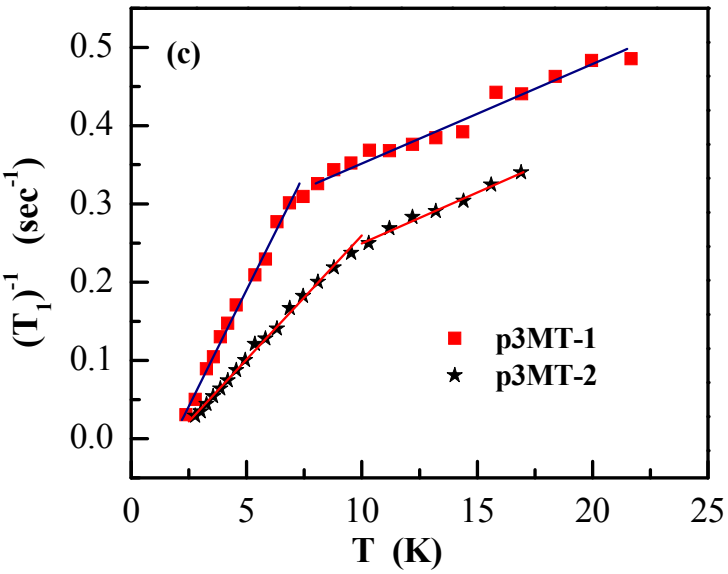

Fig.9c: ^{19}F-T_1 dependence of temperature at 9.0 T. Solid line is fit to the modified Korringa relation expressed by Eq. (3).

The fits for ^{1}H-T_1 data to Eq. (3) yield straight lines, though the lines does not pass through the origin, as shown in Figures9(a,b& c). In conventional Korringa behavior the fit is supposed to pass through the origin, unlike the present case. The change in slopes is related to the change in Knight shift which in turn is related to the EEI and disorder. An important feature of these fits is the following: (1) it shows a positive intercept, which implies a finite relaxation time at T → 0 K, and this is attributed to the EEI contribution to

the relaxation mechanism and (2) the rapid decrease in the positive intercept implies that the relaxation mechanism is becoming considerably weak as T → 0 K. The value of S_K from the fit to Eq. (3) is shown in Table III. The ^{1}H-T_1 data for T < 50 K and at 0.9 T is shown in Fig. 9.a.

The change in slope is observed only in case of p3MT-2, since the number of conduction electrons is less, the relaxation process has slowed down considerably, unlike in case of p3MT-1. One of the important reason to carry out at high field T_1 measurement is that at the particular temperature below the value given by $T_Z = g\mu_B B/2k_B$, the local electron moment magnetization saturates, and this eliminates the contribution from SDPC to the relaxation mechanism; and this in turn makes Korringa like process as the dominant relaxation mechanism[20, 37, 47, 48]. Hence it is quite reasonable to use the modified Korringa relation to explain the low temperature (T < T_Z) T_1 data. At T > T_Z, the fits to Eq. 3, yield the values of S_K (see Table III) in the range of 1-15, which is quite reasonable.

Interestingly, in p3MT-2 an increase in slope in ^{1}H-T_1 at 0.9 T is observed below 6 K; while in p3MT-1, it is not observed till 2.5 K. This is due to the fact that in p3MT-2 the number of conduction electrons is less than that in p3MT-1; and this increases theinteraction among the localized spins, resulting in a freeze-out of spin diffusion to paramagnetic centers (SDPC) at higher temperature.

Table III. S_K values at different fields and temperatures.

Samples	Field	S_K values	
		S_{K1} (T > T_Z)	S_{K2} (T < T_Z)
p3MT-1	0.9 T (^{1}H)	68.86	
	9.0 T(^{1}H)	14.33	205
	9.0 T (^{19}F)	18.91	88.05
	16.4 T (^{1}H)	1.514	61.75
	23.4 T (^{1}H)	1.211	34.16
p3MT-2	0.9 T (^{1}H)	49.11	755.76[a]
	9.0 T (^{19}F)	19.31	47.07

[a] : T < 6 K, not T < T_Z.

In case of ^{19}F (at 9 T) the increase in T_1 occurs at the same temperature for both p3MT-1 and p3MT-2.However, the S_K values for T< T_Z, as shown in the inset of Fig. 9.b, are rather large (34-205) indicating deviations from the Korringa relation. Furthermore, the S_K values

vary inversely with field, suggesting that the field-induced localization of carriers is reducing the contribution arising from EEI to S_K. Also the S_K values (~ 19) for ^{19}F-T_1 data at $T > T_Z$, as in Fig. 9.c, is similar to that observed in ^{1}H-T_1 data; and at $T < T_Z$ the data show deviation. The S_K value for p3MT-1 is higher than that in p3MT-2, since the contributions from both EEI and disorder are larger in former case. Hence both the ^{1}H-T_1 and ^{19}F-T_1 data consistently show that role of EEI is quite significant in the values of S_K and the relaxation mechanism at low temperatures. Nevertheless these large values for S_K at low temperatures indicate that the model (as in Eq.3) is not fully satisfactory to take into account the roles of both disorder and EEI.

From the above analysis (C.2.1.a and C.2.2), we can explain the observation of faster relaxation rate of ^{1}H (below 150 K) in p3MT-1 than for p3MT-2 (section 3.B.2) as follows. Above 50 K the relaxation is due to the reorientation of the symmetric sub groups. In conducting polymers, the rigidity of the chains increases at higher doping level and this restricts the degrees of freedom for the reorienting groups. Also, the presence of larger number of dopants in p3MT-1 hinders the reorientation of the CH_3 groups as the potential barriers increase.This results in a decrease of $1/T_1$, provided that τ_c for the CH_3 rotation decreases due to the increase in the potential barrier corresponding to the increased number of PF_6 groups. Further below 50 K, the reorientational motions of symmetric groups like CH_3 and PF_6 tend to freeze. However, a finite relaxation time has been observed below 50 K, indicating the possibility for other mechanisms, and this is largely due to the relaxation via the conduction electrons. Here the fluorines are relaxed via spin diffusion to the methyl group protons, which in turn are relaxed to the lattice via conduction electrons. Since more number of PF_6 is present in p3MT-1, more fluorines relax via spin diffusion to protons, hence the $1/T_1$ in p3MT-1 is less than that in p3MT-2.

Combining the analysis of C.2.1.b and C.2.2, one can explain the observation of crossover in ^{19}F-T_1^{-1} between p3MT-1 and p3MT-2 (section 3.B.5). Although the reorientational motion of PF_6 groups is the dominant relaxation mechanism at higher temperatures in both samples, the PF_6 groups in p3MT-2 are relatively free to reorient, since the chains in p3MT-1 are more rigid, as discussed before. However, below T < 25 K the relaxation of fluorine via the methyl protons to the conduction electrons seems to occur faster in p3MT-1 due to the availability of larger number of conduction electrons compared to p3MT-2; and this mechanism becomes more relevant when the activated reorientational motions are frozen.

A comparison of the ^{19}F – T_1^{-1} and ^{1}H-T_1^{-1} can give an insight into the inter-chain and intra-chain relaxation mechanisms. Since PF_6 is sandwiched between the polymer chains, ^{19}F nuclei, thus can relax on either side of the polymer chain. However, ^{1}H relaxation mechanism can occur mainly along the chain, as protons are attached to the polymer backbone.

The ^{19}F – T_1^{-1} data in Fig. 4b show the cross over between p3MT-1 and p3MT-2 samples at T ~ 25 K. However such a crossover has not been observed in the ^{1}H-T_1^{-1} measurements. These data indicate that a systematic investigation of both ^{1}H and ^{19}F

relaxation mechanism can probe the inter chain versus intra chain relaxation mechanism. However, these results warrant more detailed investigation in the future.Thus the analysis of relaxation time in p3MT samples shows that ^{1}H-T_1 can be a good probe to monitor the intra chain mechanism while ^{19}F-T_1 (NMR nuclei in the dopant) can probe the inter chain processes.

It is interesting to discuss the T_1 data at 9.0 T, 16.3T and 23.4 T below T_Z. $(T_1T)^{-1}$ vs T data (Fig. 4c and 4d) at these fields show pinning of paramagnetic centres at 0.6 K, 6.04 K, 11.02 K and 15.72 K for 0.9T, 9.0 T, 16.4 T and 23.4 T respectively. Hence, modified Korringa relation with EEI and disorder will dominate the relaxation mechanism with a positive slope below the corresponding temperatures, while above these temperatures modified Korringa relation with SDPC, EEI and disorder with a negative slope will be the relaxation mechanism upto the highest temperature of experiment.

As discussed in the experimental section, from the equilibrium amplitudes of the proton and fluorine FID signals, it was found that the dopant concentration in p3MT-1 is two orders of magnitude higher than that from p3MT-2. The dc conductivity data also has shown that p3MT-1 has higher conductivity than p3MT-2. The N(E_F) calculation from susceptibility data also shows that, its value in p3MT-1 is two orders higher than p3MT-2. This shows that there is an internal consistency in the data analysis.

3.D. Comparison with the metallic PPy-PF_6

It is interesting to compare the results in p3MT with similar studies[13] in metallic PPy-PF_6. In latter, the relaxation below 6 K follows modified Korringa relation, while at intermediate temperature (6 < T < 50 K) and high temperature (T > 50 K) the relaxation is due SDPC and reorientation of PF_6 groups, respectively. One of the important differences between the two systems is that the conductivity pPy-PF_6 is large (~ 150 S/cm) even at 20 mK, while in fully doped p3MT-1 the conductivity changes by two orders of magnitude from room temperature down to 77 K, and at very low temperature the conductivity is quite low as in typical insulators. Proton and fluorine T_1 measurements show some common features: (i) reorientation of PF_6 groups, (ii) SDPC followed by modified Korringa relation, as shown in Fig. 10. In pPy-PF_6 the protons, that are bound to the main chain, are relaxed due to the reorientation of PF_6 groups; while in p3MT-1 the proton relaxation is due to both CH_3 and PF_6 groups. The main difference is that the enhancement factor in S_K in p3MT samples at low temperature is quite high, which shows a large deviation from the Korringa relation, unlike in metallic pPy-PF_6 films.

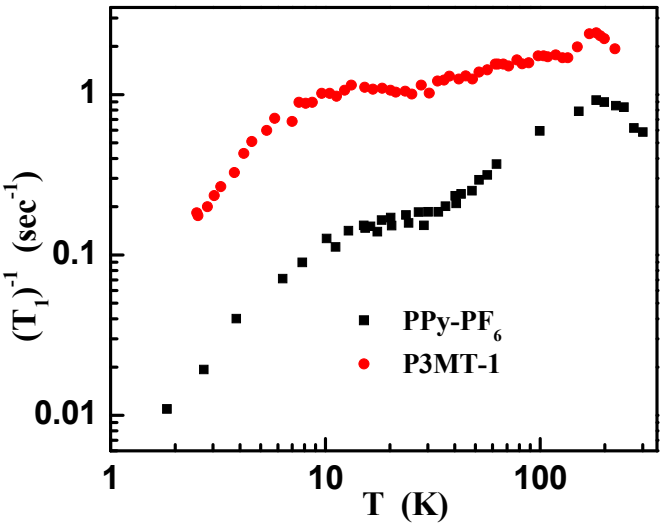

Fig. 10.Comparison of ^{1}H-T_1 between metallic PPy-PF_6 and p3MT-1.

Present study also shows the cross over in ^{19}F relaxation as a function of temperature in doped and dedoped samples. This indicates that ^{19}F (NMR nuclei in the dopant) T_1^{-1} measurements can be used to probe inter-chain conduction mechanism, while ^{1}H probes the intra-chain conduction mechanism.

4. Conclusions

Conductivity, magnetic susceptibility and NMR T_1 (proton and fluorine) measurements have been carried out in both fully doped and dedopedp3MT samples. Conductivity of both p3MT samples decreases by two orders of magnitude at 77 K. Magnetic susceptibility data show the presence of both Curie and Pauli spins. The number of Pauli spins in p3MT-1 is two orders of magnitude larger than that in p3MT-2. Measurements of proton and fluorine NMR T_1 show that the reorientation of the symmetric subgroups like CH_3 and PF_6 is the dominant relaxation mechanism at low frequency and higher temperatures. Three different types of relaxation mechanism have been identified in these systems. Relaxation at high temperatures is due to the reorientation of symmetric sub groups. In the intermediate temperature region, the relaxation mechanism is dominated by the SDPC followed by modified Korringa relaxation and at very low temperature ranges deviations from Korringa like relaxation is observed. Present high field and low temperature measurements show that relaxation through paramagnetic centres can be pinned at any given temperature depending on the magnitude of the field. Further this work clearly signifies that the same system can show different dimensionality depending upon the window (temperature and frequency) of observation.

Acknowledgement:

The authors thank DST-NSF for financial assistance to carry out this work. The work at Los Alamos was performed under the auspices of the US Department of Energy, Office of Science. The work done by the UCLA authors was supported by NSF Grants DMR-0334689 and OISE-0225578. The work at the NHMFL Tallahassee received the financial support from the National Science Foundation under cooperative agreement DMR-0084173 and the State of Florida.

References:

[1] N. Bloembergen,Physica,**15,** 588 (1949).

[2] G. SachsandE. Dormann,Synth. Met.,**25,** 157 (1988).

[3] A. C. Kolbert, S.Caldarelli, K.F.Their, N. S.Sariciftci, Y. Cao andA. J. Heeger,Phys. Rev. B,**51,**1541 (1995).

[4] L. K. Alexander, N.Büttgen, R.Nath, A.V.Mahajan and A.Loidl,Phys. Rev. B,**76,** 064429 (2007).

[5] A. Narath and D. C. Barham, Phys. Rev.,**176,** 476 (1968).

[6] J.Szeftel andH.Alloul, J. Non-cryst. Solids,**29,** 253 (1978).

[7] T. L. Reinecke and K. L.Ngai, Phys. Rev. B,**12,** 3476(1975).

[8] A. Avogadro, F.Tabak, M.Cortiand F.Borsa, Phys. Rev. B,**41,** 6137 (1990).

[9] P. W. Anderson, B. I. Halperin and C. M. Varma, Phil. Mag. 25, 1, (1972)

[10] W.A. Phillips, J. Low Temp. Phys. 7, 351, (1972)

[11] J. Korringa,Physica,**16,** 601 (1950).

[12] B. S. Shastry and E. Abrahams,Phys. Rev. Lett.,**72,** 1933 (1994).

[13] K. J. Singh, W. G. Clark, K. P. Ramesh and M. Reghu,J. Phys. Cond. Matt.,**20,** 465208 (2008).

[14] M. Nechtschein, F.Devreux, R. L.Greene, T. C. Clark and G. B. Street, Phys. Rev. Lett.,**44,** 356 (1980)

[15] K. Mizoguchiand K.Kume, Solid State Comm.,**89,** 971 (1994).

[16] G. Soda, D. Jerome, M.Weger, J. M. Fabreand L.Giral, Solid State Comm.,**18,** 1417 (1976).

[17] W. Hoptner, M.Mehring, J. U. Von Schutz, H. C. Wolf, B. S. Mora, V.Enkelmann and G.Wegner, Chem. Phys.,**73**, 253 (1982).

[18] A. Kaiser, B. Pongs, G.Fischer and E.Dormann, Phys. Lett. A,**282**, 125 (2001).

[19] S. Masubuchi, T.Fukuharaand S.Kazama, Synth. Met.,**84**, 601 (1997).

[20] M.Nechtschein, Handbook of Conducting Polymers 2nd revised and expanded ed.M. Dekker (New York), 141 (1998).

[21] R. Menon,Handbook of Conducting Organic Conductive Molecules and Polymer ed. H. S. Nalwa, (New York: Wiley) **4**, 47 (1997).

[22] N. S. Sariciftci, A. J.Heeger and Y.Cao, Phys. Rev. B.,**49,** 5988 (1994).

[23] Y. Long, Z.Chen, J.Shen, Z.Zhang, L.Zhang, H.Xiao, M.Wan and J. L.Duvail, J. Phys. Chem. B, **110**, 23228 (2006).

[24] H. S. Nalwa, J. Polym. Sci: Part C: PolymLett.,**26,** 351 (1988).

[25] P. K. Kahol, Phys. Rev. B, **62,** 13803 (2000).

[26] P. K. Kahol, J. C. Ho, Y. Y.Chen, C. R.Wang, S.Neeleshwar, C. B.Tsai and B.Wessling,Synth. Met.,**151,** 65 (2005).

[27] F.Moraes, D.Davidov, M. Kobayashi, T. C.Chung, J.Chen, A. J.Heeger and F.Wudl, Synth. Met.,**10,** 169 (1985).

[28] R. S. Kohlman, J.Joo and A. J. Epstein, Physical Properties of Polymers Handbook ed. J. E. Mark 459 (1996).

[29] G. Sachs, E.Dormann and M. Schwoerer, Solid State Comm.,**53,** 73 (1985).

[30] K. Mizoguchi, F. Shimizu and K. Kume, Synth. Met.,**41,** 185 (1991).

[31] J. Wieland, U.Haeberlen, D.Schweitzer and H. J. Keller, Synth. Met.,**19,** 393 (1987).

[32] B. Bloembergen, N.Purcell and R. V. Pound, Phys. Rev. **73,** 679 (1948).

[33] A.Kaiser, B. Pongs, G. Fischer and E.Dormann, Phys. Lett. A, **282,** 125 (2001).

[34] G. Nemec, V.Illich and E.Dorman, Synth. Met.,**95,**149 (1998).

[35] C. H. Tso, J. D. Madden and C. A. Michal, Synth. Met.,**157,**460 (2007).

[36] E. C. Reynhardt, S. Jurgaand K.Jurga, Chem. Phys. Lett.,**194,** 410 (1992).

[37] A. Abragam,The principal of Nuclear magnetism Oxford university press (1991).

[38] N. Bloembergen,Physica,**15,** 386 (1949).

[39] M. Sutirtha, K. P. Ramesh, R. Kannan and J. Ramakrisna, Phys. Rev. B,**70,** 224202 (2004).

[40] C. P. Slichter, Principles of Magnetic Resonance 3rd edition. (Heidelberg: Springer), 156 (1989).

[41] A. Narath and H. T.Weaver, Phys. Rev.,**175,** 373 (1968).

[42] W. S. Robert Jr. and W. W. Warren Jr.,Phys. Rev. B,**3,** 1562 (1971).

[43] G. Soda, D. Jerome, M.Weger, J.Alizon, J.Gallice, H.Robert, J. M.Fabre andL.Giral, J. Phys. (Paris),**38,** 931 1977.

[44] K. F. Their, C. Goze, M. Mehring, F. Rachdi, T. Yildrim and J. E. Fischer, Phys. Rev. B,**59,**10536 (1999)

[45] M. Mehring, Low dimensional conductors and superconductors, ed. D. Jerome and L. S. Caron (New York: Plenum Press) 185 (1987).

[46] D. Köngeter and M.Mehring, Phys. Rev. B,**39,** 6361 (1989).

[47] E. R. Andrew,Nuclear Magnetic Resonance (Cambridge University Press) 192 (1955).

[48] W. G. Clark, K.Tanaka, S. E.Brown, R.Menon, F. Wudl, W. G.Moulton andP. Kuhns, Synth.Met.,**101,** 343 (1999).